ISCIES'11

Proceedings of ISCIES'11
2nd International Symposium on
Computational Intelligence for Engineering Systems

Instituto Superior de
Engenharia de Coimbra

Coimbra, Portugal
16-18 November, 2011
http://www.iscies11.ipc.pt

isep Instituto Superior de
Engenharia do Porto

gecad
Grupo de Investigação em Engenharia
do Conhecimento e Apoio à Decisão

ISEL
INSTITUTO SUPERIOR
DE ENGENHARIA DE LISBOA

IEEE
PORTUGAL SECTION

IEEE
Computational
Intelligence
Society
Portugal Chapter

Multidimensional Scaling Analysis of Robotic Signals

Miguel F. M. Lima
Department of Electrical Engineering
School of Technology, Polytechnic Institute of Viseu
Viseu, Portugal
e-mail: lima@mail.estv.ipv.pt

J. A. Tenreiro Machado
Department of Electrical Engineering
Institute of Engineering, Polytechnic Institute of Porto
Porto, Portugal
email: jtm@isep.ipp.pt

Abstract—**This paper analyzes the signals captured during impacts and vibrations of a mechanical manipulator. To test the impacts, a flexible beam is clamped to the end-effector of a manipulator that is programmed in a way such that the rod moves against a rigid surface. Eighteen signals are captured and several metrics are calculated between them, such as the correlation, the mutual information and the entropy. A sensor classification scheme based on the multidimensional scaling technique is presented.**

Keywords: *signals; robotics; correlation; mutual information; entropy; MDS*

I. INTRODUCTION

The robotic manipulators have several sensors and actuators in order to carry out the desired movements. Due to the multiplicity of sensors, the data obtained can be redundant because the same type of information may be seen by two or more sensors. Due to the price of the sensors, this aspect can be considered in order to reduce the cost of the system. On the other hand, the placement of the sensors is an important issue in order to obtain the suitable signals of the vibration phenomenon. Moreover, the study of these issues can help in the design optimization of the acquisition system. In this line of thought a sensor classification scheme is presented.

Several authors have addressed the subject of the sensor classification scheme. White [1] presents a flexible and comprehensive categorizing scheme that is useful for describing and comparing sensors. The author organizes the sensors according to several aspects: measurands, technological aspects, detection means, conversion phenomena, sensor materials and fields of application. Michahelles and Schiele [2] systematize the use of sensor technology. They identified several dimensions of sensing that represent the sensing goals for physical interaction. A conceptual framework is introduced that allows categorizing existing sensors and evaluates their utility in various applications. This framework not only guides application designers for choosing meaningful sensor subsets, but also can inspire new systems and leads to the evaluation of existing applications.

Today's technology offers a wide variety of sensors. In order to use all the data from the diversity of sensors a framework of integration is needed. Sensor fusion, fuzzy logic, and neural networks are often mentioned when dealing with problem of combing information from several sensors to get a more general picture of a given situation. The study of data fusion has been receiving considerable attention [3–4]. A survey of the state of the art in sensor fusion for robotics can be found in [5]. Henderson and Shilcrat [6] introduced the concept of logic sensor that defines an abstract specification of the sensors to integrate in a multisensor system.

The recent developments of micro electro mechanical sensors (MEMS) with unwired communication capabilities allow a sensor network with interesting capacity. This technology was applied in several applications [7], including robotics. Cheekiralla and Engels [8] propose a classification of the unwired sensor networks according to its functionalities and properties.

This paper presents a development of a sensor classification scheme based on a statistical metrics using the multidimensional scaling technique (MDS).

Bearing these ideas in mind, this paper is organized as follows. Section 2 describes briefly the robotic system enhanced with the instrumentation setup. Section 3 presents a review of the main concepts involved in the experiments and section 4 shows the experimental results. Finally, section 5 draws the main conclusions and points out future work.

II. EXPERIMENTAL PLATFORM

The developed experimental platform has two main parts: the hardware and the software components [9]. The hardware architecture is shown in Fig. 1. Essentially it is made up of a robot manipulator, a personal computer (PC), and an interface electronic system.

The interface box is inserted between the robot arm and the robot controller, in order to acquire the internal robot signals; nevertheless, the interface captures also external signals, such as those arising from accelerometers and force/torque sensors. The modules are made up of electronic cards specifically designed for this work. The function of the modules is to adapt the signals and to isolate galvanically the robot's electronic equipment from the rest of the hardware required by the experiments.

The software package runs in a Pentium 4, 3.0 GHz PC and, from the user's point of view, consists of two applications: the acquisition application and the analysis package. The acquisition application is a real time program
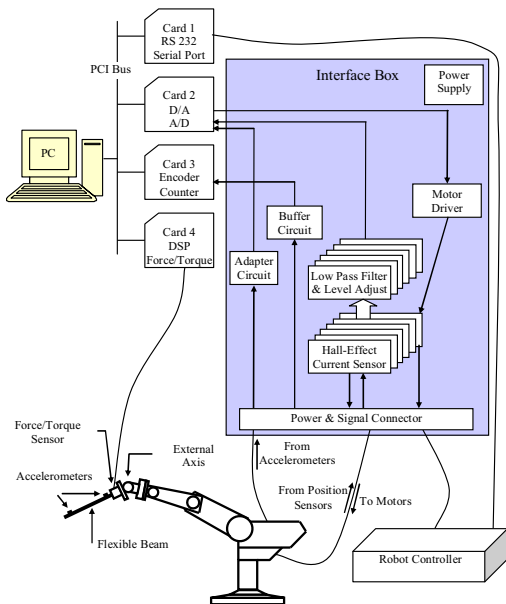
Figure 1. Block diagram of the hardware architecture.

for acquiring and recording the robot signals.

After the real time acquisition, the analysis package processes the data off-line in two phases, namely, pre-processing and processing. The preprocessing phase consists of the signal selection in time, and their synchronization and truncation. The processing stage implements several algorithms for signal processing algorithms such as, the auto and cross correlation, Fourier transform (FT), window Fourier transform, time synchronization, etc.

III. MAIN CONCEPTS

This section presents a review of the fundamental concepts involved in the experiments such as the multidimensional scaling (MDS) and metrics in the time domain, namely the correlation, the mutual information and the entropy.

A. Multidimensional scaling

The MDS has its origins in psychometrics and psychophysics where is used as a tool for perceptual and cognitive modeling. From the beginning MDS has been applied in many fields, such as psychology, sociology, anthropology, economy, educational research, etc. In last decades this technique has been applied also in others areas, including computational chemistry [10], machine learning [11], concept maps [12] and wireless network sensors [13].

MDS is a generic name for a family of algorithms that construct a configuration of points in a low dimensional space from information about inter-point distances measured in high dimensional space. The new geometrical configuration of points, which preserves the proximities of

the high dimensional space, allows gaining insight in the underlying structure of the data and often makes it much easier to understand.

The problem addressed by MDS can be stated as follows: given n items in a m–dimensional space and an $n \times n$ matrix of proximity measures among the items, MDS produces a p-dimensional configuration X, $p \le m$, representing the items such that the distances among the points in the new space reflect, with some degree of fidelity, the proximities in the data. The proximity measures the (dis)similarities among the items, and, in general, it is a distance measure: the more similar two items are, the smaller their distance is. The Minkowski distance metric provides a general way to specify distance for quantitative data in a multidimensional space:

$$d_{ij} = \left(\sum\nolimits_{k=1}^{m} w_k \left| x_{ik} - x_{jk} \right|^r \right)^{1/r} \qquad (1)$$

where m is the number of dimensions, x_{ik} is the value of dimension k for object i and w_k is a weight. For $w_k = 1$, with $r = 2$, the metric equals the Euclidian distance metric, while $r = 1$ leads to the city-block (or Manhattan) metric. In practice, normally the Euclidian distance metric is used but there are several others definitions that can be applied, including for binary data [14].

Typically MDS is used to transform the data into two or three dimensions, and visualizing the result to uncover hidden structure in the data, but any $p \le m$ is also possible. A rule of thumb to determine the maximum number of m, is to ensure that there are at least twice as many pairs of items then the number of parameters to be estimated, resulting in $m \ge 4p + 1$ [15]. The geometrical representation obtained with MDS is indeterminate with respect to translation, rotation, and reflection [16].

There are two forms of MDS: metric MDS and nonmetric MDS. The metric MDS uses the actual values of dissimilaries, while nonmetric MDS can use only their ranks. Metric MDS assumes that the dissimilarities δ_{ij} calculated in the original m–dimensional data and distances d_{ij} in the p–dimensional space are related as follows $d_{ij} \approx f(\delta_{ij})$, where f is a continuous monotonic function. Metric (scaling) refers to the type of transformation f of the dissimilarities and its form determines the MDS model. If $d_{ij} = \delta_{ij}$ (it means $f = 1$) and a Euclidian distance metric is used we obtain the classical (metric) MDS.

In metric MDS the dissimilarities between all objects are known numbers and they are approximated by distances. Thus objects are mapped into a low dimensional space, distances are calculated, and compared with the dissimilarities. Then objects are moved in such way that the fit becomes better, until an objective function is minimized. In the context of MDS this objective function is called

stress.

In nonmetric MDS, the metric properties of f are relaxed but the rank order of the dissimilarities must be preserved. The transformation function f must obey the monotonicity constraint $\delta_{ij} < \delta_{rs} \Rightarrow f(\delta_{ij}) \leq f(\delta_{rs})$ for all objects. The advantage of nonmetric MDS is that no assumptions need to be made about the underlying transformation function f. Therefore, it can be used in situations that only the rank order of dissimilarities is known (ordinal data). Additionally, it can be used in cases which there are incomplete information. In such cases, the configuration X is constructed from a subset of the distances, and, at the same time, the other (missing) distances are estimated by monotonic regression.

In nonmetric MDS it is assumed that $d_{ij} \approx f(\delta_{ij})$, therefore $f(\delta_{ij})$ are often referred as the disparities [17–18], in contrast to the original dissimilarities δ_{ij}, on one hand, and the distances d_{ij} of the configuration space, on the other hand. In this context, the disparity is a measure of how well the distance d_{ij} matches the dissimilarity δ_{ij}.

There is no rigorous statistical method to evaluate the quality and the reliability of the results obtained by an MDS analysis. However, there are two methods used often for that purpose: The Shepard plot and the stress. The Shepard plot [19] is a scatterplot of the dissimilarities and disparities against the distances, usually overlaid with a line with a unitary slope. The Shepard plot provides a qualitative evaluation of the goodness of fit, while the stress value gives a quantitative evaluation. Additionally, the stress plotted as a function of dimensionality can be used to estimate the adequate p–dimension. When the curve ceases to decrease significantly we found an "elbow" that may correspond to a substantial improvement in fit.

Beyond the aspects referred before, there are others developments of MDS that includes the replicated MDS and weight MDS. The replicated MDS allows the analysis of several matrices of dissimilarity data simultaneously. The weighted MDS generalizes the distance model as defined in (1).

B. Metrics in the time domain

Several indices can be used to evaluate the relashionship between the signal, including statistical, entropy and information theory approaches. These metrics are based on a bidimensional probability density function associated with the two signals $x_1(t)$ and $x_2(t)$ acquired in the same time interval and can be calculated according with the expression:

$$P(x_1, x_2) = \frac{\beta(x_1, x_2)}{\iint \beta(x_1, x_2) dx_1 dx_2} \tag{2}$$

where β is the bidimensional histogram.

The marginal probability distributions of the signals $x_1(t)$

and $x_2(t)$ are denoted as $P(x_1)$ and $P(x_2)$, respectively. The expected values, $E(x_1)$ and $E(x_2)$, and the variances, $V(x_1)$ and $V(x_2)$, are then easily obtained.

The correlation coefficient R [20] is a statistical index that provides a measurement of the similarity between two signals $x_1(t)$ and $x_2(t)$ and is define as

$$R(x_1, x_2) = \frac{E(x_1 x_2) - E(x_1)E(x_2)}{\sqrt{V(x_1)V(x_2)}} \tag{3}$$

where $E(x_1 x_2)$ is the joint expected value.

The mutual information [21–22], or transinformation [23] is the index that measures the dependence of two variables in the viewpoint of the information theory. The mutual information for the two signals $x_1(t)$ and $x_2(t)$ is:

$$I(x_1, x_2) = \log_2 \frac{P(x_1, x_2)}{P(x_1)P(x_2)} \tag{4}$$

The average mutual information between the two signals is given by:

$$I_{av}(x_1, x_2) = \iint P(x_1, x_2) \log_2 \frac{P(x_1, x_2)}{P(x_1)P(x_2)} dt dt \tag{5}$$

The entropy [21] is a statistical measure of randomness. This index applied to the two signal $x_1(t)$ and $x_2(t)$ gives the join entropy [24] between the two signal defined as:

$$H(x_1, x_2) = -\iint P(x_1, x_2) \log_2 P(x_1, x_2) dt dt \tag{6}$$

IV. EXPERIMENTAL RESULTS

In the experiments a flexible link is used that consists of a long and round flexible steel rod clamped to the end-effector of the manipulator. In order to analyze the impact phenomena in different situations two types of beams are used. Their physical properties are shown in Table 1. The robot motion is programmed in a way such that the rods move against a rigid surface. Figure 2 depicts the robot with the flexible link and the impact surface.

During the motion of the manipulator the clamped rod is moved by the robot against a rigid surface. An impact occurs and several signals are recorded with a sampling frequency of $f_s = 500$ Hz. The signals come from several sensors, such as accelerometers, force and torque sensor, position encoders, and current sensors.

Figure 2. Steel rod impact against a rigid surface.

TABLE 1 PHYSICAL PROPERTIES OF THE FLEXIBLE BEAMS.

Characteristics	Thin rod	Gross rod
Material	Steel	Steel
Density [kg m^{-3}]	4.34×10^3	4.19×10^3
Mass [kg]	0.107	0.195
Length [m]	0.475	0.475
Diameter [m]	5.75×10^{-3}	7.9×10^{-3}

In order to have a wide set of signals captured during the impact of the rods against the vertical screen thirteen trajectories were defined. Those trajectories are based on several points selected systematically in the workspace of the robot, located on a virtual Cartesian coordinate system (see Fig. 3). This coordinate system is completely independent from that used on the measurement system. For each trajectory the motion of the robot begins in one of these points, moves against the surface and returns to the initial point. A paraboloid profile was used for the trajectories.

A. Robotic signals

Figures 4 to 7 depict some of the signals corresponding to the cases: (*i*) without impact, (*ii*) the impact of the rod on a gross screen and (*iii*) the impact of the rod on a thin screen using either the thin or the gross rod.

Due to space limitations only the most relevant signals are depicted. In this example, the signals present clearly a strong variation at the instant of the impact that occurs, approximately, at $t = 3$ s. Consequently, the effect of the impact forces (Fig. 4) and moments (Fig. 5) is reflected in the current required by the robot motors (Fig. 6). Moreover, as would be expected, the amplitudes of forces due to the gross screen (case *ii*) are higher than those corresponding to the thin screen (case *iii*). On the other hand, the forces with the gross rod (Fig. 4 *b*) are higher than those that occur with the thin rod (Fig. 4 *a*). The torques present also an identical behavior in terms of its amplitude variation for the tested conditions (see Fig. 5).

Figure 7 presents the accelerations at the rod free-end (accelerometer 1), where the impact occurs, and at the rod clamped-end (accelerometer 2). The amplitudes of the accelerometers signals are higher near the rod impact side. Furthermore, the values of the accelerations obtained for the thin rod (Fig 7 *a*) are higher than those for the gross rod (Fig 7 *b*), because the thin rod is more flexible.
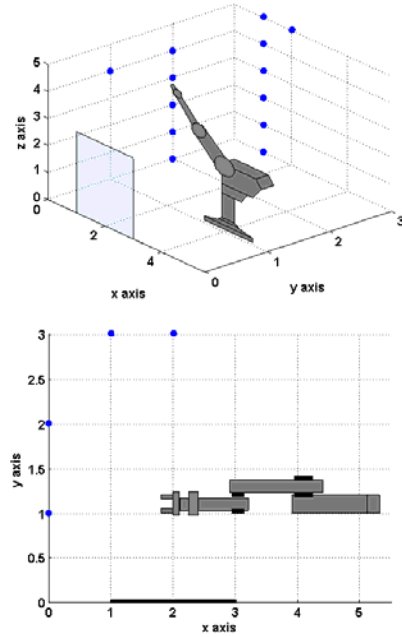

Figure 3. Schematic representation {3D, 2D} of the robot and the impact surface on the virtual cartesian coordinate system.
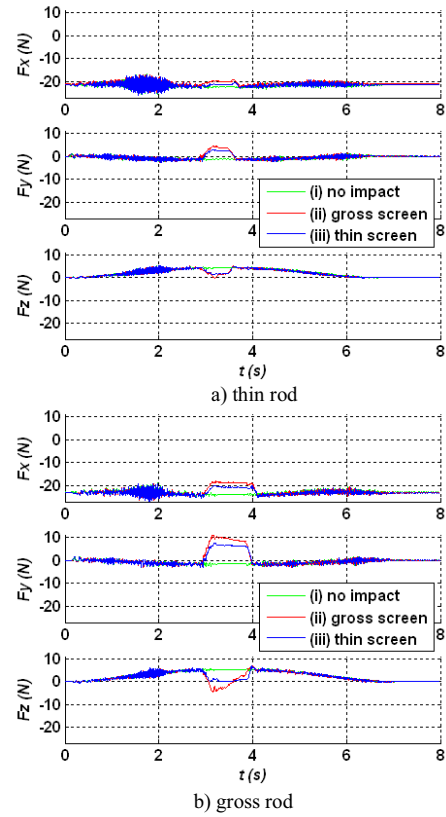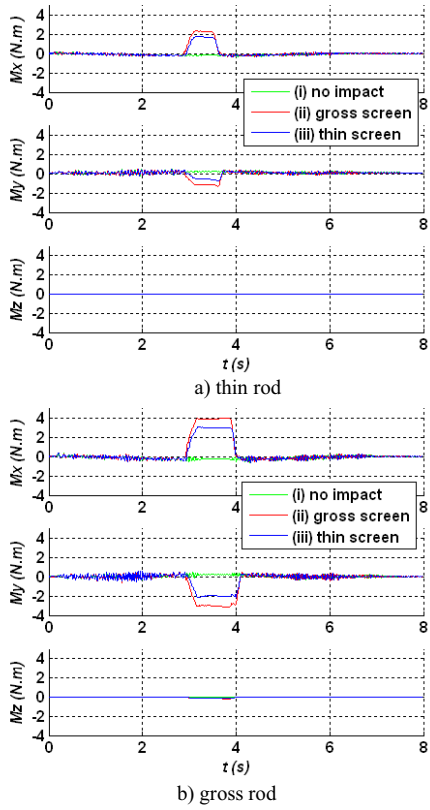

a) thin rod

b) gross rod

Figure 4. Forces at the gripper sensor.

a) thin rod

b) gross rod

Figure 5.   Moments at the gripper sensor.

a) thin rod

b) gross rod
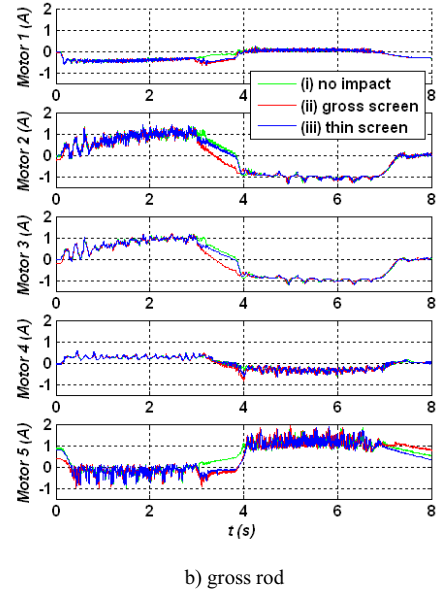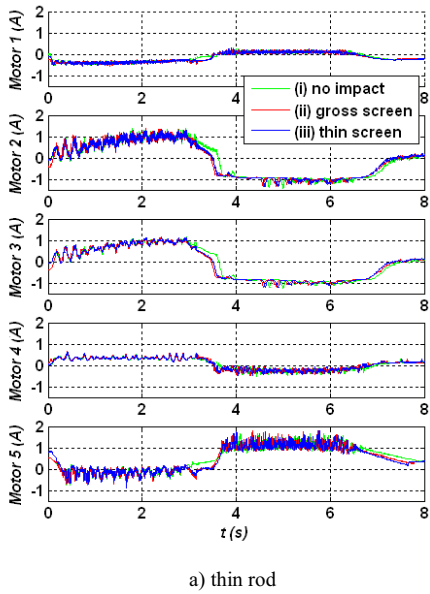
Figure 6.   Electrical currents of the robot's axes motors.
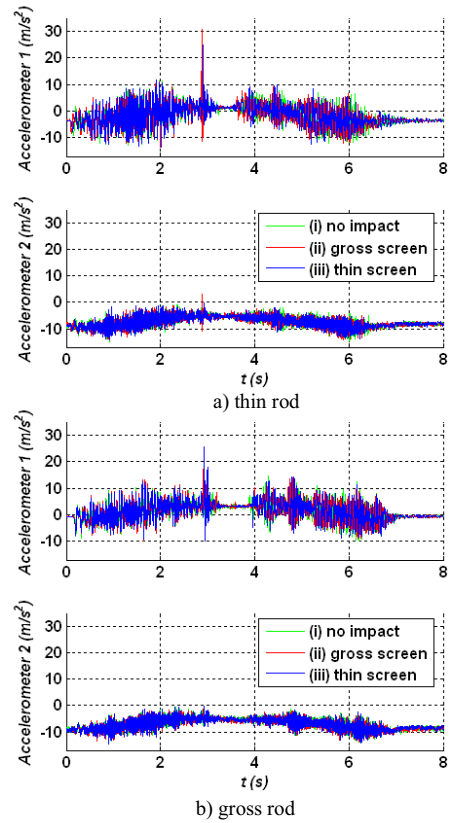

a) thin rod

b) gross rod

Figure 7.   Rod accelerations.

B. Metrics applied to the signals

Figure 8 *a*) shows the squared correlation coefficient R^2 between the signals captured during the same impact trajectory, for an experiment in the case of (*i*) using the gross rod. The results obtain with R^2 are simetric relative to the diagonal formed by $R^2(x_i, x_j)$ for $i = j$, where the metric is maximum, as expected. To clearly visualize the results only one side is shown. The correlation between the same families of signals is higher than the correlation between different families. For example, the correlation between the currents and positions are low. The same occurs between the currents and the forces, moments and accelerations. It exists a strong correlation between the positions and the forces, moments and accelerations that depends, as expected, on the trajectory.
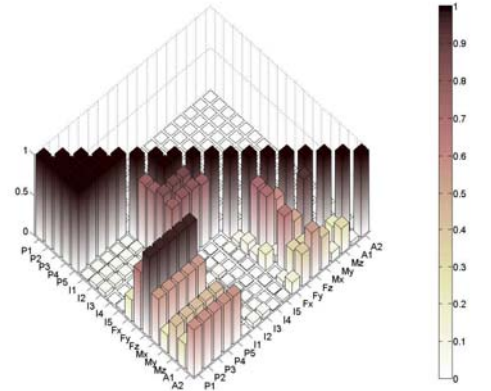
Figure 8 *b*) shows the average mutual information between the signals for the same experiment used previously for the correlation. Again the results obtain with $I_{av}(x_1, x_2)$ are simetric relative to the diagonal where the metric is maximum. Due to the same reason referred before only one side is shown. The values presented are normalized. The values of the index $I_{av}(x_1, x_2)$ between the positions are high.

Figure 8 *c*) shows a chart based on the entropy between the signals for the same experiment used previously for the other metrics. In fact, the values shown are proportional to the inverse of the index $H(x_1, x_2)$ due to the normalization used. Again, the values of this index between the positions are high.

The metrics shown in figure 8 were obtained for an experiment corresponding to one trajectory. In future this approach should be applied for all the thirteen trajectories referred before.

C. MDS Analysis

In order to reveal some hypothetical hidden relationships between the signals the MDS technique is used. Several metric and non-metric scaling MDS criteria were tested. The Sammon [25] metric scaling criterion revealed good results for the correlation. This criterion gives weight to small distances, which helps to detect clusters. On the other hand, for the tests developed, the stress metric scaling criterion, normalized with the sum of squares of the dissimilarities, is the best choice for the mutual information and entropy. Therefore, the referred criteria are adopted in this work. In Fig. 9 is shown the 2–D (*a*) and 3–D (*b*) locus of sensor positioning based on the correlation measure between the signal for the case (*i*) using the gross rod. Three groups of signals can be defined. The ellipses depicted in the chart represent two of these groups. The positions $\{P_1, P_2, P_3, P_4, P_5\}$ signals are located close to each other. The electrical currents $\{I_1, I_2, I_3, I_4, I_5\}$ are situated on the left of the chart and near each other. Finally, the remaining signals form a big group composed by the forces $\{F_x, F_y, F_z\}$, moments $\{M_x, M_y, M_z\}$ and the accelerations $\{A_1, A_2\}$ situated at scattered positions away from each other.
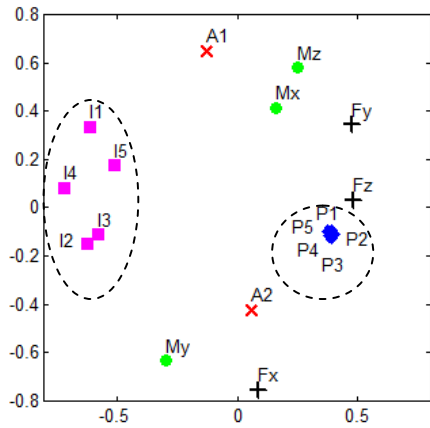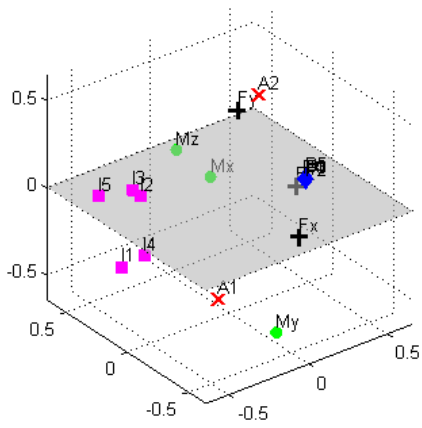

a) Correlation
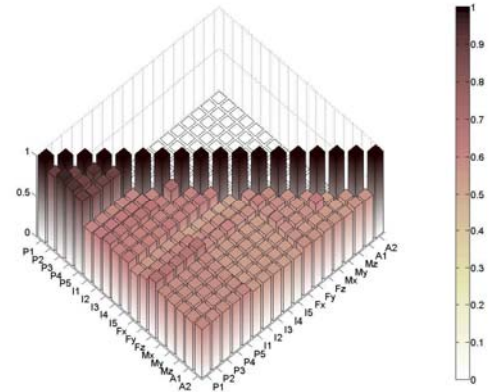
b) Average mutual information
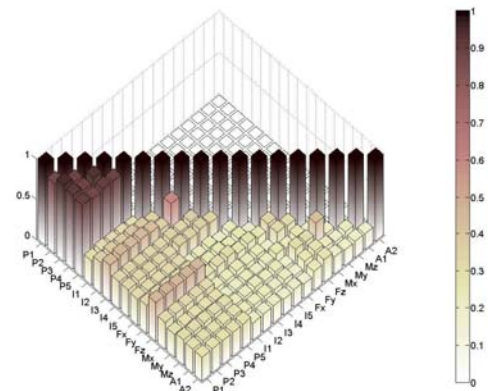
c) Entropy

Figure 8. Metrics between the signals for the case (*i*) using the gross rod.
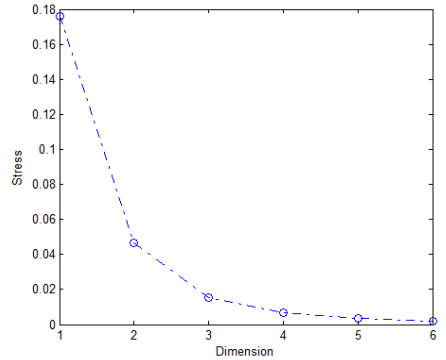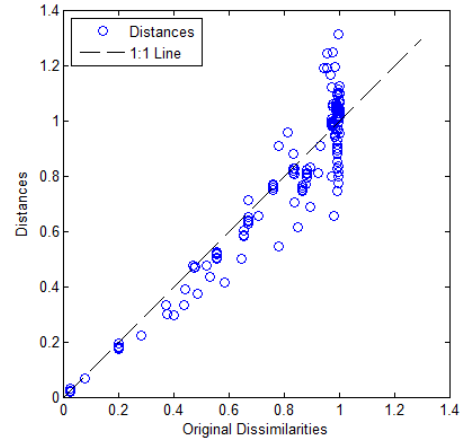
a)

b)

Figure 9.   Locus of sensor positioning based on the correlation measure between the signals for the case (*i*) using the gross rod: 2D (a); 3D (b).

Fig. 10 shows two tests developed to evaluate the consistency of the results obtained by MDS analysis. The value of the stress function *versus* the dimension is shown in Fig. 10 (a), which allows the estimation of the adequate *p*–dimension. An "elbow" occurs at dimension three for a low value of stress, which corresponds to a substantial improvement in fit. Additionally, the Shepard plot (Fig. 10 b) shows the fitting of the 3–D configuration distances to the dissimilarities.

Fig. 11 shows the 2–D locus of sensor positioning based on the average mutual information measure between the signal for the case (*i*) using the gross rod. The 2–D spatial presentation of the MDS is shown due to clarity in the interpretation. Once more three groups of signals can be defined. Again, the positions $\{P_1, P_2, P_3, P_4, P_5\}$ signals are located close to each other and the electrical currents $\{I_1, I_2, I_3, I_4, I_5\}$ are situated on the left of the chart and near each other. Finally, the remaining signals form a big group

a)

b)

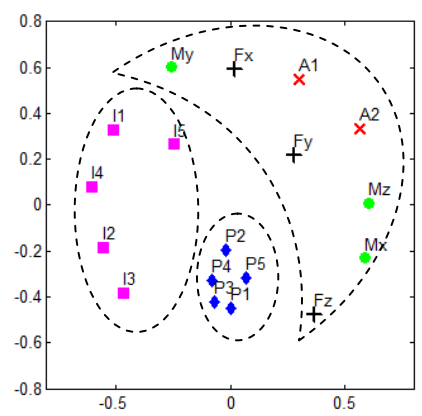Figure 10. Evaluation of MDS results based on correlation: Stress test (a); Shepard plot (b)

Figure 11. 2–D Locus of sensor positioning based on the average mutual information measure between the signals for the case (*i*) using the gross rod.

composed by the forces $\{F_x, F_y, F_z\}$, moments $\{M_x, M_y, M_z\}$ and the accelerations $\{A_1, A_2\}$ situated at scattered positions

at top right region. Fig. 12 shows the stress test (a) and the Shepard plot (b) of the 3–D MDS based on the average mutual information. From the stress test we can see that low values of stress are achieved only for high dimensions, which could reveals that the 2–D or 3–D dimensions are not suitable for representing the locus of the variables. Additionally, the Shepard plot shows the inappropriate fitting of the 3–D configuration distances to the dissimilarities. This plot indicates that this metric solution is probably not suitable, because it shows both a nonlinear pattern and a large scatter. The former implies that many of the largest dissimilarities would tend to be somewhat exaggerated in the visualization, while moderate and small dissimilarities would tend to be understated. The latter implies that distance in the visualization would normally be a poor evidence of dissimilarity. In particular, a good fraction of the large dissimilarities would be badly understated.

Fig. 13 shows the 2–D locus of sensor positioning based on the join entropy measure between the signals for the same case of the previous examples. Again, the 2–D spatial presentation of the MDS is shown due to clarity in the interpretation. The locus of the variables is similar to that obtained for the average mutual information metric. Fig. 14
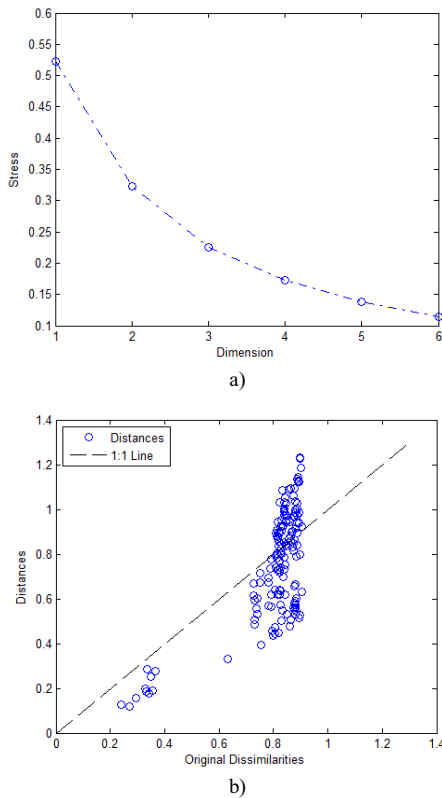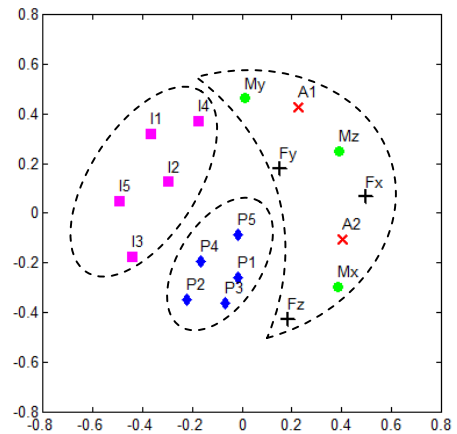

Figure 13. 2–D Locus of sensor positioning based on the join entropy measure between the signals for the case (*i*) using the gross rod.
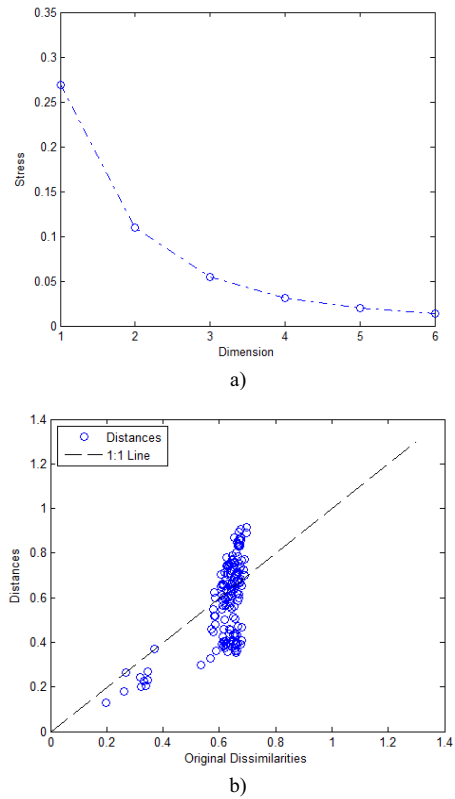

a)

b)

Figure 14. Evaluation of MDS results based on the join entropy: Stress test (a); Shepard plot (b)

shows the stress test (a) and the Shepard plot (b) of the 3–D MDS based on the join entropy. From the stress test we can see once more that low values of stress are achieved only for high dimensions, which could reveals that the 2–D or 3–D dimensions are not suitable for representing the locus of the variables. Moreover, the Shepard plot shows the

a)

b)

Figure 12. Evaluation of MDS results based on the average mutual information: Stress test (a); Shepard plot (b)

inappropriate fitting of the 3–D configuration distances to the dissimilarities.

In conclusion, from the experiments analyzed for all the three metrics studied, the MDS gives a spatial representation of the signals that can be classified in three groups. However, the tests developed to evaluate the consistency of the results obtained by MDS show that the correlation metric seems to be more appropriate when comparing with the average mutual information and entropy.

V. CONCLUSION

In this paper an experimental study was conducted to investigate several robot signals. A new sensor classification strategy based on MDS was proposed. The adopted methodology revealed hidden relationships between the robotic signals and leads to arrange them in three groups.

The results merit further investigation as they give rise to new valuable concepts towards instrument control applications. In this line of thought, in future, we plan to pursue several research directions to help us further understand the behavior of the signals. The classification presented was obtained for an experiment corresponding to one trajectory. In future this approach should be applied for all the thirteen trajectories referred before.

REFERENCES

[1] R. M. White. A sensor classification scheme. *IEEE Trans. on Ultrasonics, Ferroelectrics and Frequency Control*, 34(2):124–126, 1987.

[2] F. Michahelles and B. Schiele. Sensing opportunities for physical interaction. *Workshop on Physical Interaction (PI03) at Mobile HCI*, Udine, Italy, 2003.

[3] Jaime Esteban, Andrew Starr, Robert Willetts, Paul Hannah, and Peter Bryanston-Cross. A review of data fusion models and architectures: towards engineering guidelines. *Neural Computing & Applications*, 14(4):273–281, 2005.

[4] R. C. Luo and M. G. Kay. A tutorial on multisensor integration and fusion. In *IEEE 16th Annual Conf. of Industrial Electronics Society*, pages 707–722, 1990.

[5] J. K. Hackett and M. Shah. Multi-sensor fusion: a perspective. In *Proc. IEEE Int. Conf. on Robotics & Automation*, pages 1324–1330, 1990.

[6] Henderson, T. C., and E. Shilcrat, Logical sensor systems. J. of Robotic Systems, vol. 1, no. 2, pp. 169-193, 1984.

[7] Arampatzis, Th Lygeros, J. Manesis, S., A Survey of Applications of Wireless Sensors and Wireless Sensor Networks, Proc. IEEE Int. Symp. on Intelligent Control, pp. 719-724, 2005.

[8] Cheekiralla, S., D.W. Engels, A functional taxonomy of wireless sensor network devices, Auto ID Laboratory, MIT, Cambridge, USA.

[9] Miguel F. M. Lima, J.A. Tenreiro Machado, Manuel Crisóstomo, Experimental Set-Up for Vibration and Impact Analysis in Robotics, in *WSEAS Trans. on Systems*, Issue 5, vol. 4, May, 2005, pp. 569-576.

[10] Glunt, W., Hayden, T. L., Raydan, M. (1993). *Molecular conformation from distance matrices*. J. Computational Chemistry, 14, 114-120.

[11] Tenenbaum, J., de Silva, V., Langford, J. (2000). *A global geometric framework for nonlinear dimensionality reduction*. Science, 290(5500), 2319-2323.

[12] Martinez–Torres, M., BarreroGarcia, F., ToralMarin, S., Gallardo, S. (2005). *A Digital Signal Processing Teaching Methodology Using Concept-Mapping Techniques*, IEEE Transactions on Education, Volume 48, Issue 3, Aug. 2005 Page(s): 422 – 429 DOI:10.1109/TE.2005. 849737.

[13] Mao, Guoqiang, Fidan, B. (2009). *Localization Algorithms and Strategies for Wireless Sensor Networks,Igi-Global,* ISBN 978-1-60566-397-5 (ebook).

[14] Cox, T., Cox, M. (2001). Multidimensional scaling, 2nd edition, Chapman & Hall/CRC, ISBN 1584880945.

[15] Carreira-Perpinan, M. (1997). *A review of dimension reduction techniques*. Technical report CS-96-09, Department of Computer Science, University of Shefield.

[16] Fodor, I. (2002). *A survey of dimension reduction techniques*, Technical Report, Center for Applied Scientific Computing, Lawrence Livermore National Laboratory.

[17] Kruskal, J., Wish, M. (1978). *Multidimensional Scaling*, Newbury Park, CA: Sage Publications, Inc.

[18] Martinez, W., Martinez, A. (2005). Exploratory Data Analysis with MATLAB, Chapman & Hall/CRC Press UK, ISBN 1-58488-366-9.

[19] Shepard, R. (1962). The analysis of proximities: multidimensional scaling with an unknown distance function, I and II, Psychometrika, 27, pp. 219-246 and pp. 219-246.

[20] Orfanidis, S. (1996). *Optimum Signal Processing. An Introduction*. 2nd Edition, Prentice-Hall, Englewood Cliffs, NJ, 1996.

[21] Shannon, C. (1948). A Mathematical Theory of Communication. The Bell System Technical Journal. July; October, Vol. 27, pp. 379-423; 623-656.

[22] Cover, T. & Thomas, J. (2006). Elements of Information Theory. John Wiley & Sons, ISBN-10 0-471-24195-4.

[23] Spataru, Al. (1970). Theorie de la Transmission de l'Information – Signaux et Bruits. Editura technical, Bucarest, Roumanie.

[24] MacKay, D. (2003). Information Theory, Inference, and Learning Algorithms. Cambridge University Press, August, ISBN 0521642981.

[25] Sammon, J. A nonlinear mapping for data structure analysis. IEEE Trans. Computers, C–18(5): 401–409, May 1969.